JOURNAL OF VIROLOGY, Apr. 2006, p. 3947–3956 Vol. 80, No. 8
0022-538X/06/$08.00+0 doi:10.1128/JVI.80.8.3947–3956.2006

Rotavirus Spike Protein VP4 Binds to and Remodels Actin Bundles of the Epithelial Brush Border into Actin Bodies†

Agnès Gardet,[1] Michelyne Breton,[1] Philippe Fontanges,[2] Germain Trugnan,[1,2]* and Serge Chwetzoff[1]*

INSERM-UPMC UMR 538, Faculty of Medicine Saint Antoine, 27 rue de Chaligny, 75012 Paris, France,[1] *and Cell Imaging Core Facilities, IFR 65, Hôpital Tenon, 4 rue de la Chine, 75020 Paris, France*[2]

Received 25 November 2005/Accepted 31 January 2006

We demonstrate here that VP4, a rotaviral protein, is able to specifically bind to bundled actin microfilaments that are subsequently profoundly remodeled into actin bodies. These cytoplasmic actin bodies do not localize within identified intracellular compartments. VP4-induced actin remodeling is similar to cytochalasin D effects with kinetics compatible with that of rotavirus infection. Actin bundles' remodeling occurs both in infected and in VP4-transfected cells and in various cell lines, indicating that this is a general property of the viral protein itself. Interestingly, in intestinal epithelial cells, which represent the natural target of rotavirus, VP4 is addressed to the apical membrane where it binds specifically to brush border actin bundles and elicits its remodeling, whereas cytochalasin D impaired all the filamentous actin. These observations indicate that these original properties of VP4 likely explain the previously described brush border alterations that follow rotavirus infection of enterocytes and may also participate to the mechanism of rotavirus final assembly.

The actin cytoskeleton represents a privileged target for microbes, since it provides means for the pathogens to move within the cell, to adapt cell morphology, functions, and dynamics to the microbe's needs. Considerable data concerning the interactions of bacterial pathogens with the actin cytoskeleton have been collected. *Salmonella* and *Shigella* spp., for example, direct their own uptake into host cells by promoting several coordinated signaling pathways that induce actin remodeling into membranes ruffles engulfing the bacteria (19). An increasing amount of data also describes various strategies used by viruses to hijack and use actin microfilaments to take the control of the cellular cytoskeleton (11). In most of the cases, viruses, such as vaccinia virus and simian virus (SV40), promote actin polymerization and use these functional microfilaments to facilitate their intracellular movements, assembly, or budding (37). Human immunodeficiency virus (HIV), Epstein-Barr virus, or baculoviruses induce cell shape changes through interactions with actin filaments (12, 35, 43). Actin has also been involved in the formation of intercellular synapses that favor intercellular virus spreading upon HIV infection (24). Actin also participates in HIV and other retroviruses (such as equine infectious anemia virus) budding (8, 56) and in baculovirus assembly (14).

Surprisingly, only few viruses have been shown to destroy actin filamentous structures. In some instance, it has been shown that virus-induced disruption of actin microfilament may facilitate virus release, as it is the case for adenovirus (22), human cytomegalovirus (25), vesicular stomatitis virus (50), and rubella virus (4).

* Corresponding author. Mailing address: INSERM-UPMC UMR 538, Faculty of Medicine Saint Antoine, 27 rue de Chaligny, 75012 Paris, France. Phone for Germain Trugnan: 33 140 01 13 70. Fax: 33 140 01 13 90. E-mail: trugnan@ccr.jussieu.fr. Phone for Serge Chwetzoff: 33 1 40 01 13 42. Fax: 33 1 40 01 13 90. E-mail: chwetzoff@caramail.com.

† Supplemental material for this article may be found at http://jvi.asm.org/.

Recent studies have suggested that rotavirus, a nonenveloped virus, may also interfere with the actin cytoskeleton (6). Rotaviruses belong to the *Reoviridae* family and are the major cause of viral gastroenteritis in young children (28). Mature virions are nearly spherical icosahedral 70- to 85-nm-diameter particles with a triple shell of proteins surrounding the genome formed by 11 segments of double-stranded RNA (40). Shortly after rotavirus infection of intestinal cells, the brush border actin cytoskeleton is disorganized (6) and the apical targeting of some brush border hydrolases is impaired (26). In order to understand the mechanisms underlying rotavirus effect on actin organization and their functional consequences on the host cells, we focused our attention on the rotavirus spike protein VP4 because this protein is the exclusive constituent of the 60 spikes sticking out of the surface of rotavirus particles that are thought to mediate primary interactions of the virus with cellular components (39, 51). This rotavirus structural protein is essential for the entry of rotavirus into cells as well as for its virulence (1). During the viral cycle, VP4 is detectable early within infected intestinal cells and specifically associates with the apical plasma membrane, within raft-type membrane microdomains, before the onset of progeny virions morphogenesis (46). VP4 is a cytosolic protein that is not found within the Golgi apparatus (27), suggesting an atypical and still unknown mechanism for its apical polarized membrane targeting. It should be pointed out that the subcellular localization of VP4 still remains a matter of debate. Some authors have shown that VP4 localized within or near the endoplasmic reticulum (ER) in nonpolarized MA104 cells (18, 36, 38). In a recent study, however, we have shown that VP4 was not detected within the ER of polarized intestinal Caco-2 cells and was independent of tunicamycin, a drug known to block early step of N-glycosylation and ER exit (13).

We show here that VP4 binds to a subset of bundled actin microfilaments and exerts a very strong, specific, and original remodeling activity leading to the formation of actin bodies. In

intestinal cells the ability of VP4 to specifically bind to microvillar actin bundles results in its targeting to the apical membrane. Later on, interactions between VP4 and brush border actin microfilaments result in a specific remodeling of this membrane, that most likely accounts for the previously observed alterations of the intestinal brush border during rotavirus infection. Our results thus provide a molecular explanation for some critical aspects of rotavirus physiopathology. The apical expression of VP4 within microvillar actin bundles may also be part of the virus strategy for its final assembly and polarized apical release from intestinal cells.

MATERIALS AND METHODS

All culture reagents were from Invitrogen (Cergy-Pontoise, France). All other chemicals, if their sources are not stated, were from Sigma-Aldrich (Saint Quentin Fallavier, France).

Cell culture. Cell lines were obtained from the American Type Culture Collection (LGC Promochem, Molsheim, France). Cos-7 (monkey kidney) cells were maintained according to the American Type Culture Collection's instructions. Caco-2 (human colon adenocarcinoma) cells were maintained in Dulbecco's modified Eagle's medium supplemented with 20% fetal calf serum, 100 U of penicillin/ml, 100 μg of streptomycin/ml, and 1% nonessential amino acids. Cells were grown in a humidified 10% CO_2 incubator at 37°C.

Plasmids and transfection experiments. The VP4 (RF strain) full-length cDNA was obtained by PCR using pBS-RF4 as a template. One primer corresponds to the 5′ end of VP4 sequence with a XbaI (underlined) site: 5′CATCTAGATG GCTTCACTCATTTATAG3′. The second primer corresponds to the 3′ end of VP4 sequence with a HindIII (underlined) site: 5′GCAAGCTTTACAAGCGA CATTGCATTATC3′. Amplicon was ligated into a pGEMT vector (Promega, Madison, WI) and then digested with XbaI and HindIII enzymes and introduced into a pTEJ8 vector (23). The pEGFP-C1-VP4 plasmid was obtained while proceeding in the same way, using a pEGFP-C1 vector from Clontech (Ozyme, Montigny le Bretonneux, France) and the following primers: 5′ATCTCGAGC TATGGCTTCACTCATTTATAG3′ and 5′GTGGATCCTTACAAGCGACAT TGC3′ including the XhoI and BamHI (respectively underlined) sites.

Thus, enhanced green fluorescent protein (EGFP) was linked to VP4 at the N-terminal end of the viral protein. EGFP is added to the N-terminal side of the protein VP4 in order to work under the same conditions as described in reference 32. Plasmid transfections in Cos-7 cells were performed using FuGene6 (Roche Diagnostics, Meylan, France) according to the manufacturer's instructions.

Plasmid transfections in Caco-2 cells were performed using 5 μg DNA and Amaxa technology (Amaxa, Koeln, Germany), an electroporation technology that allows the delivery of DNA straight into the nucleus and that was optimized notably for Caco-2 cell lines (www.amaxa.com). Nucleofected Caco-2 cells (7.5×10^5) were seeded in a 12-mm-diameter well.

Virus. Production and titration of the rotavirus RF strain were carried out as described for the RRV strain (27). Infections of cells were performed as previously described (46), with a multiplicity of infection of 1 PFU for Cos-7 cells or 10 PFU for Caco-2 cells.

Antibodies and fluorescent staining reagents. Monoclonal antibodies (MAbs) against alpha tubulin, cytokeratin, and vimentin were purchased from Sigma (Saint Quentin Fallavier, France). Polyclonal goat serum anti-actin (I-19), MAb anti-protein disulfide isomerase, and polyclonal goat serum anti-early endosome antigen 1 were from Santa Cruz (California). Polyclonal rabbit serum anti-catalase was from Biomol International (Plymouth Meeting, PA). Polyclonal sheep serum anti-TGN46 was from Serotec (Cergy-Saint-Christophe, France). MAb anti-transferrin receptor was from Zymed laboratories (Clinisciences, Montrouge, France). MAbs anti-ERGIC 53 and anti-giantin were generously provided by H. P. Hauri (Biozentrum, Basel, Switzerland). MAb anti-VP4 antibody (7.7) was a generous gift of J. Cohen (CNRS, Gif-sur-Yvette, France). Alexa 547-phalloidin was purchased from FluoProbes (Montluçon, France). Lysotracker and Mitotracker were purchased from Molecular Probes (Invitrogen, Cergy-Pontoise, France). The pDsRed2-PTS1 plasmid was from Clontech (Ozyme, Montigny le Bretonneux, France).

Immunofluorescence and confocal microscopy. For fixation, cells were quickly washed in 10 mM phosphate buffer, pH 7.4, and 150 mM NaCl (PBS) or specifically in 10 mM morpholinoethanesulfonic acid buffer [pH 6.1], 138 mM KCl, 3 mM $MgCl_2$, 2 mM EGTA, and 320 mM sucrose for microtubules preservation (41). Cells were then treated with the same buffer containing 2% paraformaldehyde for 10 min, or alternatively with ice-cold methanol for 3 min for cytokeratin fixation. After a washing, cells were further permeabilized with the starting buffer containing 0.1% Triton X-100 for 5 min.

Samples were incubated with the primary antibody for 1 h. After PBS washes, the fluorescein isothiocyanate (FITC)-, Cy3-, or Cy5-labeled second antibodies were incubated for 1 h. After washing, cells were incubated for 30 min with 100 mg/ml of 1,4-diazabicyclo-[2.2.2]-octane antifading reagent and then mounted with Glycergel (Dako, Trappes, France). For observation and analysis of living cells, a POC-Chamber-System (H. Saur, Reutlingen, Germany) was used.

The preparations were observed with a Leica TCS Spectral (SP2) instrument equipped with an inverted microscope with 63 × and 100 × oil immersion objectives both with a numerical aperture of 1.4. A krypton-argon mixed-gas laser and two helium-neon mixed-gas lasers were used to respectively generate the bands at 488 nm, 543 nm, and 633 nm.

Immunoprecipitation experiments. Infected cells were washed with ice-cold PBS, scraped in ice-cold lysis buffer containing 50 mM Tris-HCl, pH 7.5, 300 mM KCl, 5% (vol/vol) glycerol, Triton X-100 0.5% (wt/vol), and antiprotease cocktail (Roche, Meylan, France) and passed 10 times through a 23-gauge needle. After removal of nuclei by centrifugation at 400 × *g* for 10 min, clarified lysates were precleared by incubation with Dynabead paramagnetic beads covalently linked to recombinant protein A (Dynalbiotech, Compiegne, France) for 1 h at 4°C. The precleared supernatant was then subjected to immunoprecipitation overnight at 4°C, the monoclonal 7.7 anti-VP4 antibodies being covalently linked to the Dynabeads (according to the manufacturer's instructions).

The bound proteins were eluted in Laemmli sample buffer with 50 mM dithiothreitol, boiled for 5 min, and then subjected to a 12.5% sodium dodecyl sulfate-polyacrylamide gel electrophoresis.

Western blot. Immunoprecipitation experiments samples were resolved by 12.5% sodium dodecyl sulfate-polyacrylamide gel electrophoresis. After electrophoresis, proteins were transferred to an nitrocellulose membrane for immunoblot analysis. Nonspecific binding of antibodies was blocked with 1% polyvinylpyrrolidone–0.1% Tween 20 in PBS. Nitrocellulose sheets were incubated with a primary antibody for 1 h. After PBS–0.1% Tween 20 washes, horseradish peroxidase-conjugated secondary antibodies were added for 1 h. Enhanced chemiluminescence reagent and Biomax-Light 1 films (Amersham Biosciences, Saclay, France) were used for protein detection. Films were scanned with a densitometric scanner, and bands were quantified with Scion Image software (version 4.0.2).

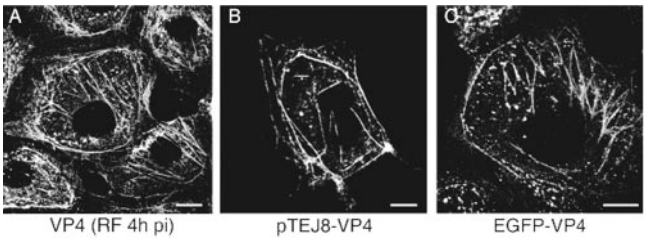

FIG. 1. VP4, the spike rotavirus protein, localizes within filaments and dots in infected and transfected Cos-7 cells. Cos-7 cells were infected with the rotavirus at 1 PFU/cell for 4 h (A) or transiently transfected with plasmids encoding VP4 (B) or EGFP-VP4 (C) for 24 h. Cells were then processed for VP4 staining (A and B). Images gallery displays projections of all 0.5-μm *xy* focal sections taken throughout the height of the cells. Scale bars = 10 μm.

RESULTS

VP4 colocalizes and coimmunoprecipitates with actin cytoskeleton. It was first observed that upon rotavirus infection of Cos-7 cells, the spike protein VP4 was detected within cells as early as 4 h postinfection (p.i.) and displayed a predominant filamentous pattern (Fig. 1A). VP4 also localized within small dots and as a faint diffuse cytosolic staining. To determine whether this distribution pattern was due to the coexpression of other viral proteins or could be ascribed to VP4 itself, Cos-7 cells were transfected with pTEJ8-VP4 and the protein was

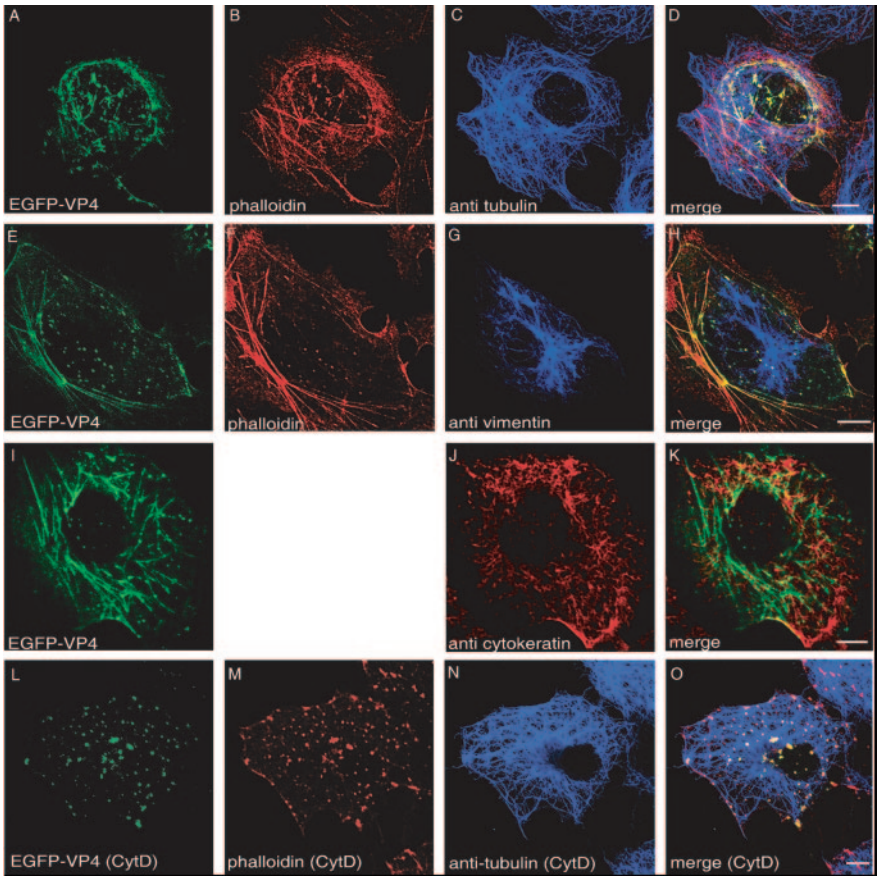

FIG. 2. EGFP-VP4 specifically colocalizes with polymerized actin. Cos-7 cells were analyzed after 24 h pEGFP-VP4 transient transfection. EGFP-VP4 expressing cells (A, E, I, and L) were immunostained with anti-α-tubulin (C and N), antivimentin (G), or anticytokeratin (J) and/or colabeled with phalloidin to detect F-actin (B, F, and M). EGFP-VP4 expressing Cos-7 cells in panels L through O were treated for 1 h with 10 μM of cytochalasin D before fixation. Images gallery displays confocal single *xy* planes. Note that colabeling of anticytokeratin and phalloidin is not possible because methanol fixation for cytokeratin preservation is not compatible with phalloidin labeling. Scale bars = 10 μm.

detected 24 h posttransfection using a monoclonal antibody (MAb 7.7) previously reported as specifically recognizing VP4 in infected cells (33). Similar results were obtained using another anti-VP4 MAb 5.73 (not shown). Preliminary unpublished experiments indicate that 7.7 MAb recognized a VP4 epitope that is not labeled early p.i. by 2G4, another MAb thought to recognize assembled VP4, suggesting that 7.7 is able to detect unassembled VP4. VP4 transfected cells displayed a pattern close to the one observed in early-infected cells (Fig. 1B). Other transfection experiments using an enhanced green fluorescent protein EGFP-VP4 chimera showed that EGFP has no deleterious effect on VP4 distribution (Fig. 1C). These data confirmed that VP4 itself contained a molecular signal sufficient to confer this filamentous distribution (33).

VP4 subcellular localization was further studied using EGFP-VP4 transiently transfected cells in which colocalization with cytoskeletal components was analyzed. These experiments showed a strong colocalization of VP4-stained filamentous structures with polymerized actin, as revealed by phalloidin staining (Fig. 2D and H). Using triple colabeling experiments, it was also shown that EGFP-VP4 did not significantly colocalize either with microtubules (Fig. 2A through D) or with vimentin (Fig. 2E through H) or cytokeratin (Fig. 2I through K). It has been previously shown that VP4 interacted with tubulin (33). Using several fixation conditions designed to optimize microtubule stability and several batches of antitubulin antibodies, we were unable to reproduce the results previously obtained. We found some colocalization between VP4 and tubulin, but this was restricted to discrete points in which both VP4 and tubulin also colocalized with actin (Fig. 2D). To confirm the predominant localization of EGFP-VP4 on the actin cytoskeleton, EGFP-VP4-expressing Cos-7 cells were treated for 1 h with 10 μM cytochalasin D, a drug known to disorganize actin microfilaments. EGFP-VP4 staining strictly colocalized with phalloidin labeling of F-actin, whereas the microtubules network remained unaffected (Fig. 2L through O). To show that a similar specific interaction between VP4 and polymerized actin also takes place during infection, VP4-stained filamentous structures were studied by colocalization experiments, using phalloidin to stain actin filaments in early-infected Cos-7 cells. As shown in Fig. 3A through C, VP4 strongly colocalized with actin microfilaments. Infected cells were also treated for 1 h with 10 μM cytochalasin D at 4 h p.i. and analyzed by immunofluorescence. As expected, upon cytochalasin D treatment, phalloidin staining was redistributed within small dots. VP4 and phalloidin staining strictly colocal-

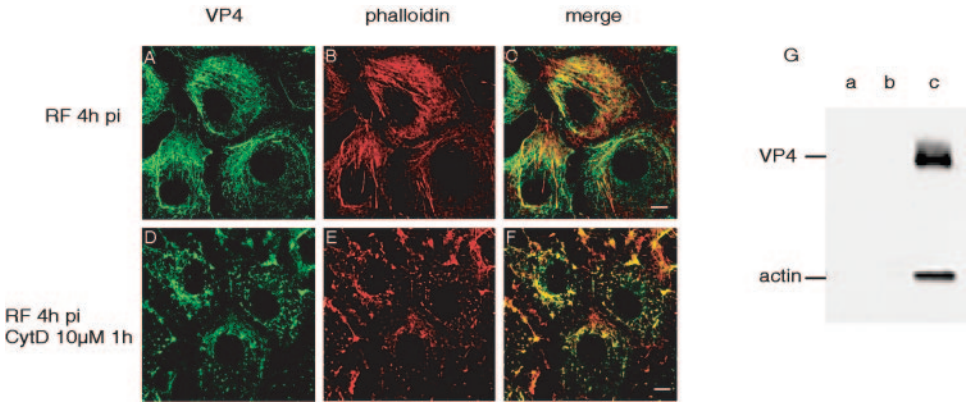

FIG. 3. VP4 and actin interact in infected Cos-7 cells. Cos-7 cells were infected with rotavirus at 1 PFU/cell for 4 h (A through C), with 1 h of 10 μM cytochalasin D treatment (D through F). Cells were then processed for phalloidin labeling (B and E) and VP4 immunostaining (A and D). Images gallery displays confocal single *xy* planes. Scale bars = 10 μm. Lysates from mock-infected or 4-h-infected Cos-7 cells were subjected to immunoprecipitation with anti-VP4 antibodies and then to Western blotting using anti-VP4 and antiactin (G). Lane a, mock-infected Cos-7 cells lysates immunoprecipitated with anti-VP4 antibodies. Lanes b and c, infected Cos-7 cells lysates immunoprecipitated with nonrelevant antibody and anti-VP4 antibodies, respectively. Note that immunoglobulins were not detected because anti-VP4 was covalently linked to protein A-Dynabeads.

ized (Fig. 3D through F), demonstrating that VP4 strongly associated with actin microfilaments. Interaction between actin and VP4 was finally assessed using a coimmunoprecipitation experiment in Cos-7 cells infected for 4 h with rotavirus. Fig. 3G shows a typical Western blot indicating that actin coimmunoprecipitated with VP4. It should be noted that were unable to coimmunoprecipitate tubulin with VP4 (not shown), a result that confirms the above-described immunofluorescence data (Fig. 2).

VP4 promotes the formation of "bodies" that do not colocalize with markers of identified intracellular compartments. VP4 not only stained filamentous structures but was also found in dots that were also labeled with phalloidin but not with antibodies against microtubules or intermediate filaments (Fig. 2). To characterize these structures in which actin was relocated upon VP4 expression, extensive colocalization studies were performed using cells transfected with EGFP-VP4 and a large panel of markers for subcellular compartments. First, the compartments of the exocytic pathway were explored using antibodies against protein disulfide isomerase for the endoplasmic reticulum, ERGIC-53 for the intermediate compartment, giantin for the Golgi apparatus and the TGN46 protein for the trans-Golgi network (Fig. 4A through D). As shown in the merged images, VP4 never colocalized with any of these compartments. Then the compartments of the endocytic pathway were explored on cells transfected with EGFP-tagged VP4 using antibodies against the early endosomal antigen-1 for early endosomes, transferrin receptor for late endosomes and Lysotracker for lysosomes (Fig. 4E through G). Again, as shown in the merged images, VP4 did not colocalize with these compartments, despite the fact that it has been recently shown to interact with Rab5 and PRA1 in the context of cell infection (16). Interestingly, interaction of VP4 with Rab5 and PRA1 was only studied at the biochemical level in infected MA104 cells and was shown to be a transient and early event (16). This may suggest either that VP4 interaction with PRA1 and Rab5 doesn't take place within endosomes or that the dynamic of this interaction cannot be observed using immunofluorescence approaches. Finally, the other main intracellular compartments were also analyzed in cells transfected with EGFP-tagged VP4 for a putative colocalization with VP4 by using Mitotracker for mitochondria and either anticatalase antibodies or a dsRed-labeled plasmid containing the peroxisome targeting signal PTS1 for peroxisomes (Fig. 4H through J). These experiments showed that VP4 did not colocalize with any of these compartments, despite the fact that it has been recently claimed that VP4 colocalized with peroxisomes (32). Our colocalization experiments were performed either on early-infected cells or on 24-h transfected cells that favor filamentous distribution of VP4 (see below), which doesn't seem to be the case in the work by Mohan et al. (32), suggesting that the images presented in this paper should correspond to late infection events. Therefore, we think that the two sets of results may describe two distinct aspects of rotavirus morphogenesis.

Together our results indicated that VP4-labeled bodies essentially contained cytoplasmic polymerized actin.

VP4 acts as an original actin-remodeling agent. The formation of actin bodies was never observed in control EGFP-transfected cells (Fig. 5A through C) and could be the consequence of an actin-remodeling event that may be promoted by VP4 expression. This hypothesis was strengthened by the observation that the formation of bodies was time dependent. As shown in Fig. 5D through G, when EGFP-VP4 expressing Cos-7 cells were observed 24 h after transient transfection, VP4 distributed within two populations of filaments and bodies that both colocalized with phalloidin. When these cells were observed 48 h after transient transfection, they displayed a different pattern in which the number of filamentous structures decreased and the number and size of bodies increased (Fig. 5H through K). This was even more pronounced 72 h after transfection (Fig. 5L through O). These bodies were strongly stained with phalloidin but not with antitubulin (Fig. 5F, J, and N) or anti-intermediate filament antibodies (not shown). The pattern of actin distribution in VP4 transfected cells was reminiscent of the one observed in normal Cos-7 cells treated with cytochalasin D. Therefore, Cos-7 cells were treated with 10

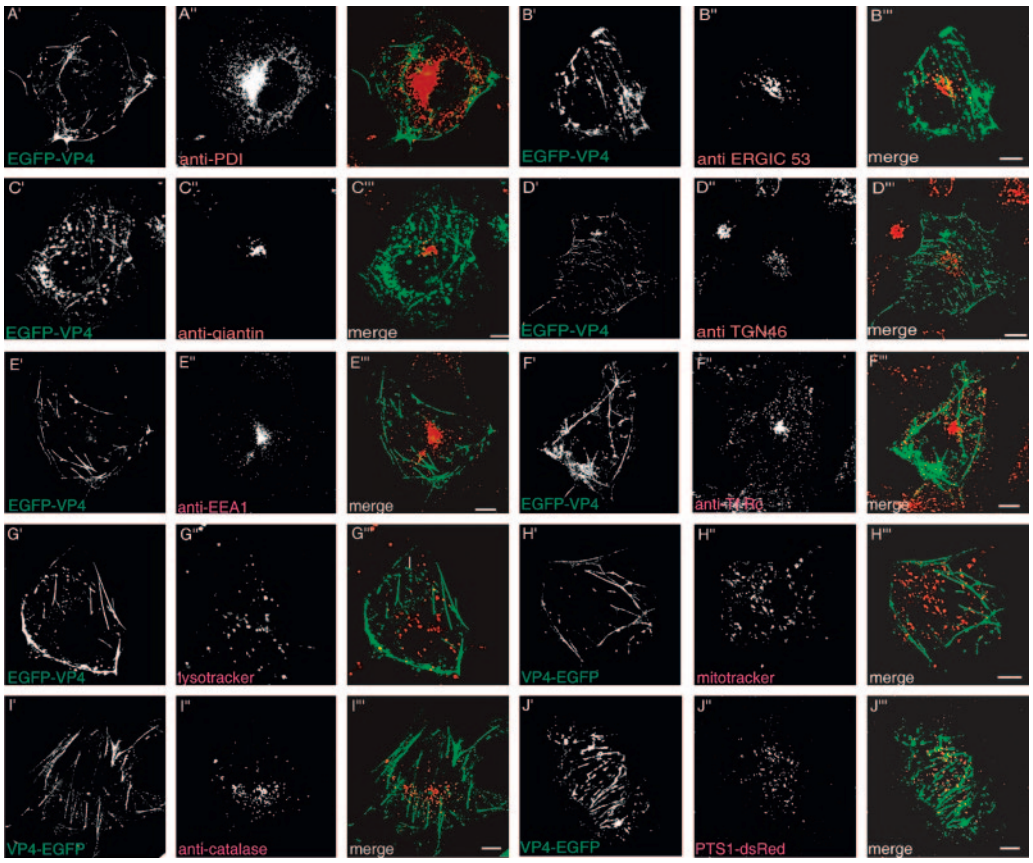

FIG. 4. EGFP-VP4 does not localize within identified vesicular compartments. Cos-7 cells were fixed after 24-h pEGFP-VP4-transient transfection, permeabilized, and vesicular compartment markers were stained by indirect immunofluorescence. The major compartments of the exocytic and endocytic pathways were explored using antibodies against protein disulfide isomerase for the endoplasmic reticulum, ERGIC-53 for the intermediate compartment, giantin for the Golgi apparatus, TGN46 protein for the trans-Golgi network, the early endosomal antigen-1 for early endosomes, transferrin receptor for late endosomes, lysotracker for lysosomes, Mitotracker for mitochondria, and either anticatalase antibodies or a dsRed-labeled plasmid containing the peroxisome targeting signal PTS1 for peroxisomes. EGFP-VP4-expressing cells (A′, B′, C′, D′, E′, F′, G′, H′, I′, and J′) were costained with anti-protein disulfide isomerase (PDI) (A"), anti-ERGIC-53 (B″), anti-giantin (C″), anti-TGN-46 (D″), anti-early endosome antigen 1 (E″), anti-transferrin receptor (F″), lysotracker (G″), mitotracker (H″), or anti-catalase (I″). (J′) displays Cos-7 cells cotransfected with plasmids encoding EGFP-VP4 and PST1-dsRed, respectively. Images gallery displays confocal single *xy* planes. Scale bars = 10 μm.

μM cytochalasin D for one hour before fixation. Confocal images displayed in Fig. 5P through R showed that the distribution of Alexa 547-phalloidin was perturbed as in VP4-transfected cells (Fig. 5, compare panels P and I). However, the protein EGFP-VP4 remodeled only actin bundles even after 72 h posttransfection, whereas 3 h cytochalasin D treatment also perturbed the microtubule organization. Additional experiments (not shown) indicated that nocodazole, a drug known to perturb microtubules, also modified actin organization when used for several hours periods, explaining why a 6-h nocodazole treatment is able to reorganize VP4 localization (33).

VP4 promotes the conversion of actin filaments into actin bodies. To directly demonstrate that VP4 promoted the conversion of actin filaments into actin bodies, time-lapse microscopy experiments were performed. EGFP-VP4 was expressed in living Cos-7 cells that were observed after 24-h transfection. As expected, EGFP-VP4 fluorescence was localized both on filaments and bodies. As shown in Fig. 6, filaments underwent a quite rapid conversion into bodies through a process that resembles contraction (see also movie S1 in the supplemental material).

VP4-induced actin-remodeling specifically alters the brush border of intestinal cells. To find out whether VP4-induced actin bundle remodeling might have functional consequences, experiments with intestinal cells were performed to analyze the brush border organization, since it has been shown that rotavirus specifically impairs the apical membrane of enterocytes (26). Caco-2 cells were transfected with pEGFP-VP4 and seeded at high cell density. At 24 h posttransfection, Caco-2 cells were not well polarized but already displayed a VP4-dependent actin bundle-remodeling (not shown). At 72 h posttransfection, Caco-2 cells displayed a polarized phenotype, and as shown in Fig. 7A through B (see also movie S1 in the supplemental material), EGFP-VP4 was expressed mostly within bodies neighboring the apical plane that strictly colocalized with phalloidin. VP4-induced actin bodies were never observed associated with stress fibers at the basal plane (Fig. 7B). VP4 apical localization was also found in rotavirus infected Caco-2 cells. At 6 h p.i., VP4 was mainly found at the

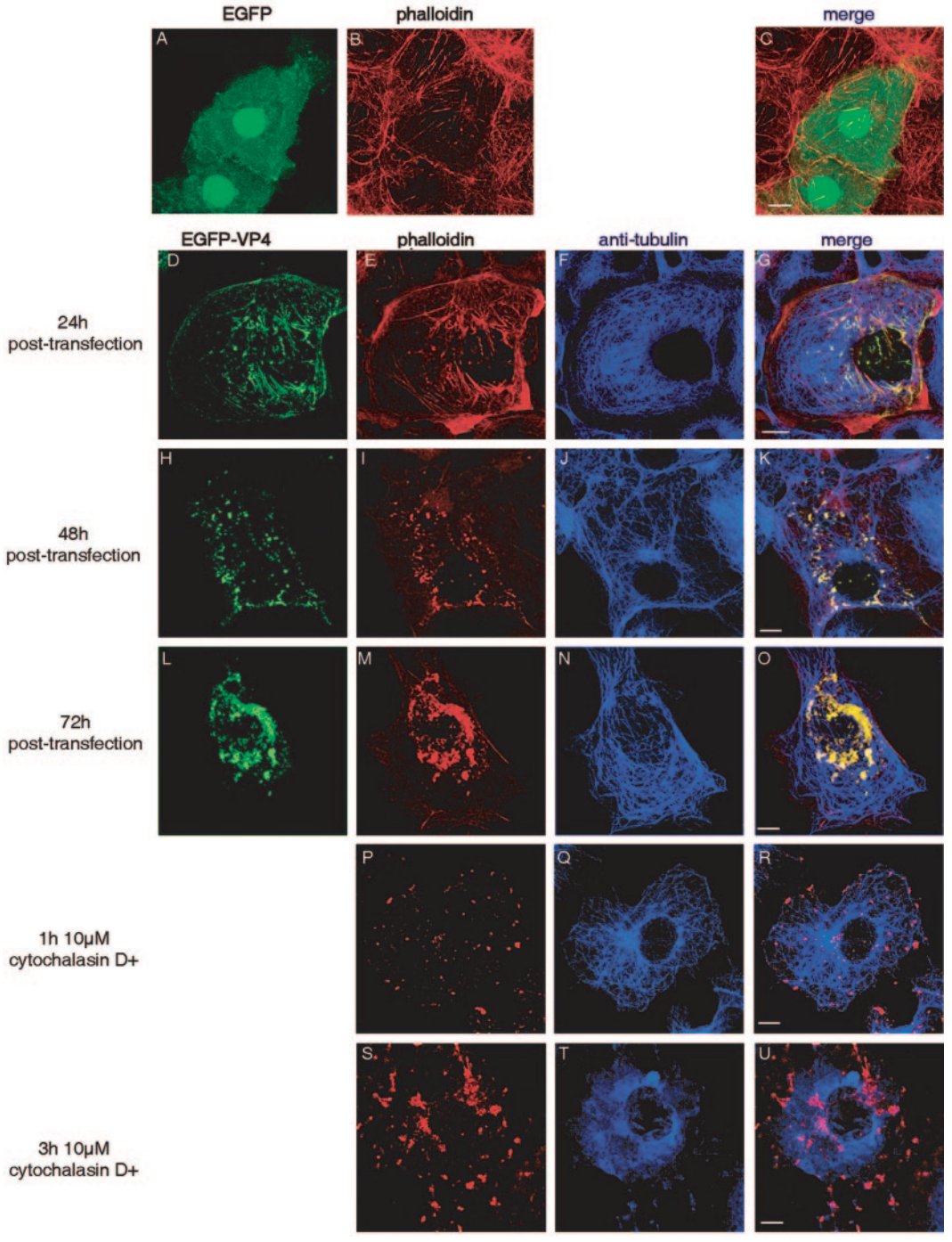

FIG. 5. VP4-induced actin remodeling partially mimics cytochalasin D. Control EGFP transfected Cos-7 cells were labeled with Alexa 547-phalloidin at 48 h posttransfection (A through C). Cos-7 cells expressing EGFP-VP4 were analyzed 24 h (D through G), 48 h (H through K) or 72 h (L through O) posttransfection. These transfected cells (A, D, H, and L) or cells treated with cytochalasin D (10 μM) for 1 h (P through R) or for 3 h (S through U) were stained using Alexa 547-phalloidin (B, E, I, M, P, and S) or anti-α-tubulin antibody (F, J, N, Q, and T). Images gallery displays projections of all 0.5-μm *xy* focal sections taken throughout the height of cells. Scale bars = 10 μm.

brush border and in the area of cell-cell junctions and strongly colocalized with F-actin (Fig. 7C through E). It is interesting that the F-actin brush border staining was inversely correlated to the intensity of VP4 staining. Actin and VP4, however, still remained strongly associated, since when cells were treated with cytochalasin D, both stainings were found to be affected and colocalized (Fig. 7F and G). Interestingly, it was noticed that cytochalasin D was able to perturb basolateral actin as well as apical actin (Fig. 7F and G), whereas VP4 was detected only at the apical plane. Later on, at 18 h p.i., all the junctional staining for both actin and VP4 had disappeared and some cells displayed a mutually exclusive distribution of these two

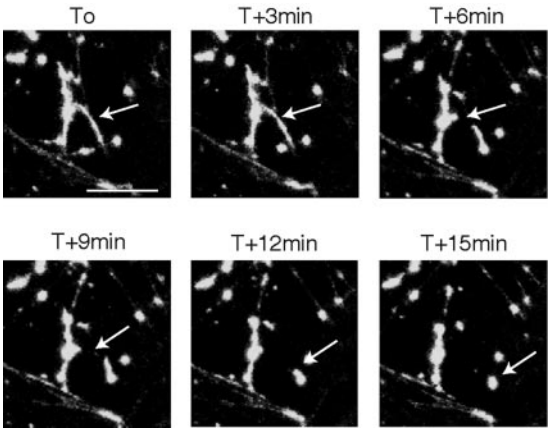

FIG. 6. VP4 remodels actin microfilaments into actin bodies. EGFP-VP4 expressing Cos-7 cells were mounted in a POC chamber and cells were perfused with 37°C 50 mM HEPES and OPTI-MEM medium. Images were acquired with a confocal microscope from time zero (To) to 15 min after perfusion (T+15min) every 3 min. Image gallery displays projections of all 0.3-μm *xy* focal sections taken throughout the height of a zoomed region of a EGFP-VP4-expressing cell. Scale bar = 10 μm.

proteins (Fig. 7H). The *xz* sections also indicated that VP4 and actin labeling are mutually exclusive at the brush border (Fig. 7I). This may be due to the fact that at this late p.i. time, a significant part of VP4 associated with other viral proteins at the brush border and may no longer be recognized by the 7.7 MAb. However, the coimmunoprecipitation experiments clearly indicated that VP4 and actin still interacted (Fig. 8), thus suggesting that a possible explanation is that the viral protein was masking a fixation site for phalloidin (Fig. 7H and I). These observations were in line with the above-described time-dependent VP4-induced actin remodeling that interestingly appeared with a rather slow kinetics that parallels the kinetics of rotavirus release from the apical membrane of intestinal cells (27).

DISCUSSION

In the present study, we show that VP4, the spike rotavirus protein, interacts with and remodels actin bundles in a very specific and original manner. Actin bundles are progressively converted into cytoplasmic actin bodies that do not localize within any identified intracellular organelles. In intestinal cells, the natural target of rotavirus, where the virus has been shown to be released in a highly polarized manner at the apical pole, VP4 localized quite exclusively within the brush border membrane in close interaction with actin microfilaments. These results have been obtained in either transfected or early-infected cells. VP4 exerts its actin-remodeling activity with kinetics consistent with those of progeny rotavirus release from the apical brush border. These results provide new data that may support both the previously described pathophysiological outcome of rotavirus infection, as well as some clues for the final steps of rotavirus assembly in intestinal cells. Thus VP4 that has already been described as an important protein for virus entry also appears as an essential protein to control its release into the apical medium. Two key properties of VP4 play a major role in the strategy developed by the virus: its ability to remodel actin microfilaments and its ability to specifically bind to microvillar actin bundles that are concentrated within the brush border of intestinal epithelial cells.

VP4 specifically remodels actin bundles into actin bodies. VP4 remodeling effects are reminiscent of the ones observed upon cytochalasin D treatment. They are actually clearly distinct. (i) In the present study, we found, like others, that a micromolar concentration of cytochalasin D was able to remodel the actin cytoskeleton within few minutes, indicating that cytochalasin D rapidly diffuses to both ends of actin microfilaments and blocks polymerization (17). The interaction of VP4 with actin is much slower and appears to be biphasic. In a first phase, starting from 9 h posttransfection, VP4 labels actin microfilaments. A similar observation is made for infected intestinal cells, in which VP4 starts to label actin microfilaments at the brush border within 4 to 6 h postinfection. This first phase likely corresponds to the time needed to synthesize enough VP4 to decorate actin microfilaments. Then, in a later phase, starting 24 h posttransfection in Cos-7 cells or 18 h postinfection in Caco-2 cells, VP4 exerts its remodeling activity, suggesting either that the intracellular concentration of VP4 became sufficient or alternatively that recruitment or induction of additional factors are required to interfere with actin bundles dynamics. (ii) VP4 exerts a very specific action on actin microfilaments with no detectable influence on other cytoskeleton components. This is not the case for cytochalasin D, since we show here that this drug, even when used for rather short periods (3 h), significantly modifies microtubule and centrosome organization. (iii) VP4 does not display any effect on the Golgi organization. It has been previously shown that, beside the well-known role of microtubule on Golgi maintenance (29, 48), disassembly of actin cytoskeleton using cytochalasin D promotes Golgi fragmentation (44). Thus, VP4 should not interact with the subset of actin microfilaments involved in Golgi maintenance. (iv) VP4 specifically destroys the brush border actin cytoskeleton in polarized epithelial cells. By contrast, cytochalasin D and other related drugs indistinctly affect most of the cellular actin cytoskeleton (7, 57). It is well known that depending on the cell type and intracellular localization, the actin cytoskeleton may adopt different types of organization such as filopodia, pseudopodia, or actin bundles that differ according to their reticulation states, their lengths and the families of associated actin binding proteins (ABPs) (42). In the present study, VP4 in either transfected or infected Caco-2 cells is essentially targeted to the apical part of the cell, where actin is organized as bundles within microvilli (21). It remains to be explained why VP4 preferentially binds to a given actin subset. Three possible mechanisms have to be considered. (i) VP4 may bind to a brush border-specific actin isoform. This proposition is based on the fact that such an isoform, namely, ACT-5, has been very recently described to be specifically involved in apical actin polymerization in the intestinal brush border of *Caenorhabditis elegans* (30). Mammalian actin isoforms specific for brush border bundles have also been described (47, 49, 54) but it remains to be explored whether VP4 may develop such specific interactions with actin isoforms in intestinal cells. (ii) It has been shown, using FRAP experiments, that actin dynamics is rather slow in epithelial brush border actin bundles (52). In contrast, actin cytoskeleton is

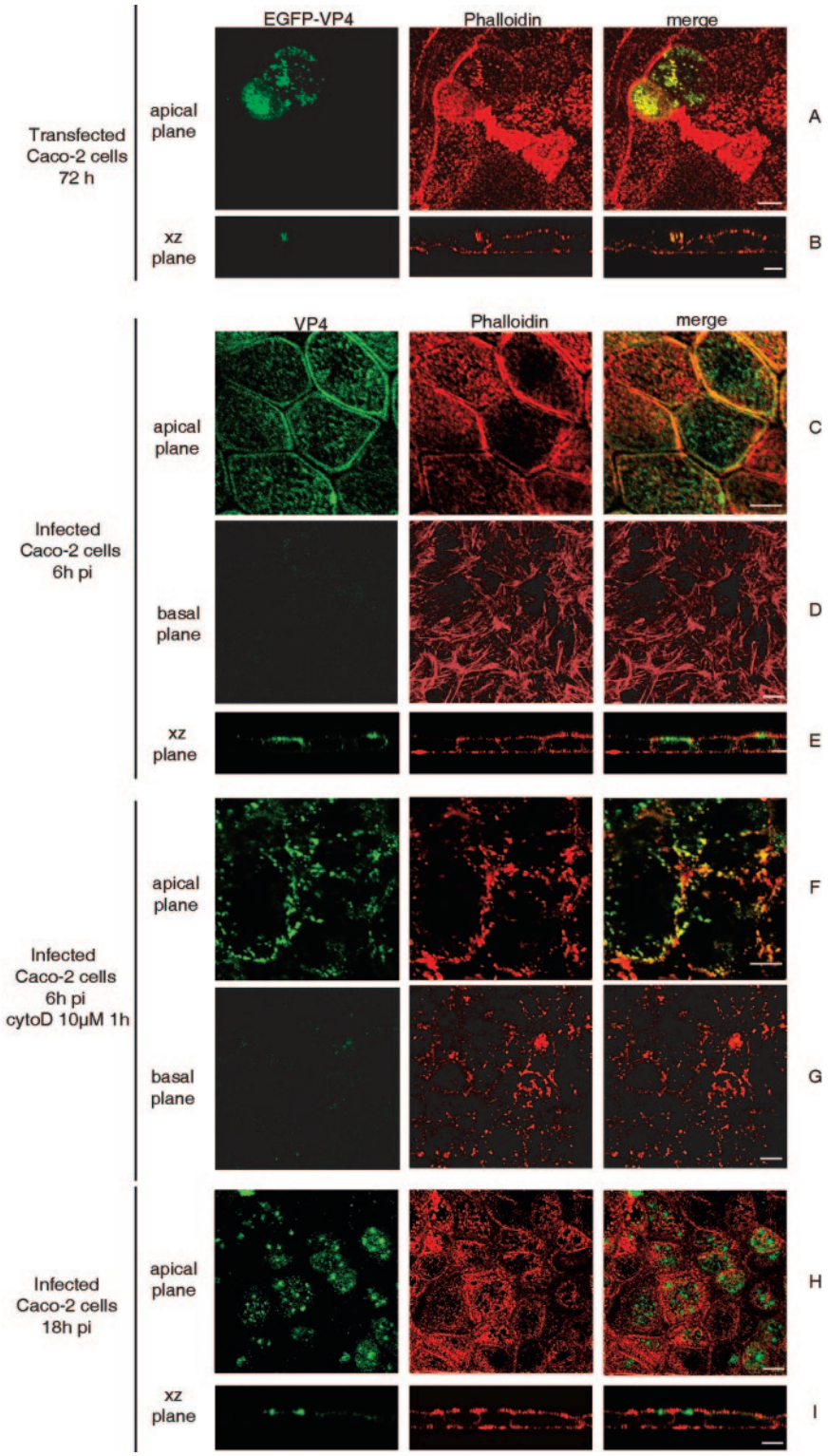

FIG. 7. VP4 localizes at the brush border and perturbs actin bundles organization. EGFP-VP4 expressing Caco-2 cells were labeled 72 h after nucleofection with Alexa 547-phalloidin. Image gallery displays an apical plane these cells (A) or *xz* section (B). Fifteen-day-old Caco-2 cells were infected with rotavirus for 6 h (C through G) or for 18 h (H and I). A 1-h cytochalasin D (cytoD) (10 μM) treatment was performed after at 5 h p.i. (F and G). Cells were then processed for Alexa 547-phalloidin labeling and VP4 immunostaining using MAb 7.7. Images gallery displays apical planes (A, C, F, and H), basal planes (D and G) or *xz* sections (B, E, and I). Scale bar = 5 μm.

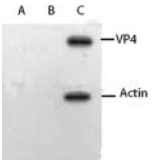

FIG. 8. Actin is coimmunoprecipitated with VP4 from 18-h-infected Caco-2 cells. Differentiated Caco-2 cells were infected with rotavirus at 10 PFU/cell. Lysates from mock-infected or 18-h-infected Caco-2 cells were subjected to immunoprecipitation with anti-VP4 antibodies and then to Western blotting using anti-VP4 and anti-actin. Lane a, mock-infected Caco-2 cells lysates immunoprecipitated with anti-VP4 antibodies; lanes b and c, infected Caco-2 cells lysates immunoprecipitated with nonrelevant antibody and anti-VP4 antibodies, respectively. Note that immunoglobulins were not detected because anti-VP4 was covalently linked to protein A-Dynabeads.

much more dynamic in structures like lamellipodia, in which actin very rapidly cycles between its polymerized and unpolymerized forms (60). Such differences in actin dynamics may influence the binding properties of VP4 in binding to actin. (iii) VP4 may interact with actin microfilaments through ABPs. There is an expanding number of proteins known to bind actin and to modify the dynamic properties of microfilaments (58). Among them, a subset of ABPs is involved in the control of actin bundle morphogenesis and dynamics that contains either cross-linking or bundling ABPs (2) or membrane linkers (5, 59). Therefore, interactions between VP4 and actin may interfere with the binding of an ABP and thus modify the fine tuning required to ensure an adequate microfilaments dynamics. Further studies are in progress to find out in an in vitro system the molecular determinants that may explain the original effect of VP4 on actin microfilaments.

Whatever the mechanisms by which VP4 interacts with actin bundles, this protein appears to be an original tool to specifically label and remodel this actin cytoskeleton subset.

Actin remodeling is essential for rotavirus infectivity. As mentioned earlier, a number of viruses required the integrity of actin microfilaments for efficient infectivity and/or viral replication. Therefore, cytochalasin D treatment frequently results in a decrease of viral infectivity for several viruses (for example, references 20 and 31). By contrast, it has been shown that a cytochalasin D treatment of rotavirus-infected MA 104 cells does not decrease its infectivity (9), which is consistent with our hypothesis. If cytochalasin D has no additional effect on the viral infectivity, it is probably because VP4 has already performed the necessary actin remodeling. The "proviral" role of actin network in rotavirus infection has also been explored on permissive and nonpermissive cell lines for this virus. Cytochalasin D was shown to transform non permissive L cells into permissive cells and to cause an increased viral infectivity. These experiments have shown that cytochalasin D had no effect on rotavirus binding and internalization by L cells but favors the completion of the virus cycle (3). We propose that this may be due to the fact that the drug would disorganize the subcortical actin cytoskeleton that normally acts as a physical barrier. Such a local disassembly of subcortical actin has been shown to be physiological and required to allow trafficking vesicles to access the membrane and favor the final steps of membrane fusion (15). In line with these observations, we propose that VP4 may use a similar strategy to perturb brush border actin and consequently favor the final step of virus assembly and release at the level of the apical pole of intestinal cells. This should not lead to an increased net virus production but simply make it possible for the virus to exit the brush border that is a highly resistant and well-organized membrane.

We previously showed that soon after infection of intestinal cells (since 4 h p.i.) and long before the assembly of new virions, VP4 is targeted to the apical membrane and is found associated with membrane microdomains enriched in cholesterol and sphingolipids, also termed rafts (46). It has also been demonstrated that other structural proteins later associate with VP4 within rafts at a time when rotaviruses start to assemble (10, 46). Together with these previous observations, the present results suggest a major role for VP4-actin interactions in the final steps of rotavirus assembly. In a first phase, actin microfilaments from the brush border may act as a reservoir for VP4 where other structural rotavirus proteins may later join to assemble as mature progeny virions. Then, in a second phase, VP4 may develop its remodeling activity, allowing a destabilization of the brush border membrane followed by rotavirus exit through a mechanism that could involve rafts. That brush border bundled actin and membrane microdomains may together play a crucial role in the final steps of apical trafficking for endogenous cellular proteins has been recently nicely demonstrated (53). Our results may thus provide a molecular explanation for a key feature of rotavirus infection in intestinal cells, i.e., brush border alterations such as shortening and constriction of the microvilli during rotavirus infection (34, 45) that may contribute both to nonlytic virus release (27) and to perturbations of epithelial functions (26, 55). To our knowledge, the peculiar VP4-induced actin microfilament remodeling described here is unique among currently identified actin-interacting proteins produced by pathogens and thus may likely represent a new viral strategy.

ACKNOWLEDGMENTS

This work was supported by institutional funding from INSERM, Ministère de la Recherche/UPMC and ACI Nanosciences. A.G. was supported by a fellowship from the French research ministry.

We acknowledge C. Sapin for the antibody production and M. Estes for critical reading of the manuscript. This work is dedicated to Jean Cohen, a friend and an outstanding scientist, who died too early.

REFERENCES

1. **Arias, C. F., P. Isa, C. A. Guerrero, E. Mendez, S. Zarate, T. Lopez, R. Espinosa, P. Romero, and S. Lopez.** 2002. Molecular biology of rotavirus cell entry. Arch. Med. Res. **33:**356–361.
2. **Bartles, J. R.** 2000. Parallel actin bundles and their multiple actin-bundling proteins. Curr. Opin. Cell Biol. **12:**72–78.
3. **Bass, D. M., M. Baylor, C. Chen, and U. Upadhyayula.** 1995. Dansylcadaverine and cytochalasin D enhance rotavirus infection of murine L cells. Virology **212:**429–437.
4. **Bowden, D. S., J. S. Pedersen, B. H. Toh, and E. G. Westaway.** 1987. Distribution by immunofluorescence of viral products and actin-containing cytoskeletal filaments in rubella virus-infected cells. Arch. Virol. **92:**211–219.
5. **Bretscher, A.** 1999. Regulation of cortical structure by the ezrin-radixin-moesin protein family. Curr. Opin. Cell Biol. **11:**109–116.
6. **Brunet, J. P., J. Cotte-Laffitte, C. Linxe, A. M. Quero, M. Geniteau-Legendre, and A. Servin.** 2000. Rotavirus infection induces an increase in intracellular calcium concentration in human intestinal epithelial cells: role in microvillar actin alteration. J. Virol. **74:**2323–2332.
7. **Cha, B., A. Kenworthy, R. Murtazina, and M. Donowitz.** 2004. The lateral mobility of NHE3 on the apical membrane of renal epithelial OK cells is limited by the PDZ domain proteins NHERF1/2, but is dependent on an intact actin cytoskeleton as determined by FRAP. J. Cell Sci. **117:**3353–3365.
8. **Chen, C., O. A. Weisz, D. B. Stolz, S. C. Watkins, and R. C. Montelaro.** 2004. Differential effects of actin cytoskeleton dynamics on equine infectious anemia virus particle production. J. Virol. **78:**882–891.

9. **Cuadras, M. A., C. F. Arias, and S. Lopez.** 1997. Rotaviruses induce an early membrane permeabilization of MA104 cells and do not require a low intracellular Ca^{2+} concentration to initiate their replication cycle. J. Virol. **71:** 9065–9074.
10. **Cuadras, M. A., and H. B. Greenberg.** 2003. Rotavirus infectious particles use lipid rafts during replication for transport to the cell surface in vitro and in vivo. Virology **313:**308–321.
11. **Cudmore, S., I. Reckmann, and M. Way.** 1997. Viral manipulations of the actin cytoskeleton. Trends Microbiol. **5:**142–148.
12. **Dawson, C. W., G. Tramountanis, A. G. Eliopoulos, and L. S. Young.** 2003. Epstein-Barr virus latent membrane protein 1 (LMP1) activates the phosphatidylinositol 3-kinase/Akt pathway to promote cell survival and induce actin filament remodeling. J. Biol. Chem. **278:**3694–3704.
13. **Delmas, O., A. M. Durand-Schneider, J. Cohen, O. Colard, and G. Trugnan.** 2004. Spike protein VP4 assembly with maturing rotavirus requires a post-endoplasmic reticulum event in polarized caco-2 cells. J. Virol. **78:**10987–10994.
14. **Dreschers, S., R. Roncarati, and D. Knebel-Morsdorf.** 2001. Actin rearrangement-inducing factor of baculoviruses is tyrosine phosphorylated and colocalizes to F-actin at the plasma membrane. J. Virol. **75:**3771–3778.
15. **Eitzen, G.** 2003. Actin remodeling to facilitate membrane fusion. Biochim. Biophys. Acta **1641:**175–181.
16. **Enouf, V., S. Chwetzoff, G. Trugnan, and J. Cohen.** 2003. Interactions of rotavirus VP4 spike protein with the endosomal protein Rab5 and the prenylated Rab acceptor PRA1. J. Virol. **77:**7041–7047.
17. **Goddette, D. W., and C. Frieden.** 1986. Actin polymerization. The mechanism of action of cytochalasin D. J. Biol. Chem. **261:**15974–15980.
18. **Gonzalez, R. A., R. Espinosa, P. Romero, S. Lopez, and C. F. Arias.** 2000. Relative localization of viroplasmic and endoplasmic reticulum-resident rotavirus proteins in infected cells. Arch. Virol. **145:**1963–1973.
19. **Gruenheid, S., and B. B. Finlay.** 2003. Microbial pathogenesis and cytoskeletal function. Nature **422:**775–781.
20. **Haxhinasto, K., A. Kamath, K. Blackwell, J. Bodmer, J. Van Heukelom, A. English, E. W. Bai, and A. B. Moy.** 2004. Gene delivery of l-caldesmon protects cytoskeletal cell membrane integrity against adenovirus infection independently of myosin ATPase and actin assembly. Am. J. Physiol. Cell Physiol. **287:**C1125–C1138.
21. **Heintzelman, M. B., and M. S. Mooseker.** 1992. Assembly of the intestinal brush border cytoskeleton. Curr. Top. Dev. Biol. **26:**93–122.
22. **Jackson, P., and A. J. Bellett.** 1985. Reduced microfilament organization in adenovirus type 5-infected rat embryo cells: a function of early region 1a. J. Virol. **55:**644–650.
23. **Johansen, T. E., M. S. Scholler, S. Tolstoy, and T. W. Schwartz.** 1990. Biosynthesis of peptide precursors and protease inhibitors using new constitutive and inducible eukaryotic expression vectors. FEBS Lett. **267:**289–294.
24. **Jolly, C., K. Kashefi, M. Hollinshead, and Q. J. Sattentau.** 2004. HIV-1 cell to cell transfer across an Env-induced, actin-dependent synapse. J. Exp. Med. **199:**283–293.
25. **Jones, N. L., J. C. Lewis, and B. A. Kilpatrick.** 1986. Cytoskeletal disruption during human cytomegalovirus infection of human lung fibroblasts. Eur. J. Cell Biol. **41:**304–312.
26. **Jourdan, N., J. P. Brunet, C. Sapin, A. Blais, J. Cotte-Laffitte, F. Forestier, A. M. Quero, G. Trugnan, and A. L. Servin.** 1998. Rotavirus infection reduces sucrase-isomaltase expression in human intestinal epithelial cells by perturbing protein targeting and organization of microvillar cytoskeleton. J. Virol. **72:**7228–7236.
27. **Jourdan, N., M. Maurice, D. Delautier, A. M. Quero, A. L. Servin, and G. Trugnan.** 1997. Rotavirus is released from the apical surface of cultured human intestinal cells through nonconventional vesicular transport that bypasses the Golgi apparatus. J. Virol. **71:**8268–8278.
28. **Kapikian, A. Z.** 2001. A rotavirus vaccine for prevention of severe diarrhoea of infants and young children: development, utilization and withdrawal. Novartis Found. Symp. **238:**153–179.
29. **Karecla, P. I., and T. E. Kreis.** 1992. Interaction of membranes of the Golgi complex with microtubules in vitro. Eur. J. Cell Biol. **57:**139–146.
30. **MacQueen, A. J., J. J. Baggett, N. Perumov, R. A. Bauer, T. Januszewski, L. Schriefer, and J. A. Waddle.** 2005. ACT-5 is an essential *Caenorhabditis elegans* actin required for intestinal microvilli formation. Mol. Biol. Cell **16:**3247–3259.
31. **Misinzo, G., P. Meerts, M. Bublot, J. Mast, H. M. Weingartl, and H. J. Nauwynck.** 2005. Binding and entry characteristics of porcine circovirus 2 in cells of the porcine monocytic line 3D4/31. J. Gen. Virol. **86:**2057–2068.
32. **Mohan, K. V., I. Som, and C. D. Atreya.** 2002. Identification of a type 1 peroxisomal targeting signal in a viral protein and demonstration of its targeting to the organelle. J. Virol. **76:**2543–2547.
33. **Nejmeddine, M., G. Trugnan, C. Sapin, E. Kohli, L. Svensson, S. Lopez, and J. Cohen.** 2000. Rotavirus spike protein VP4 is present at the plasma membrane and is associated with microtubules in infected cells. J. Virol. **74:**3313–3320.
34. **Osborne, M. P., S. J. Haddon, A. J. Spencer, J. Collins, W. G. Starkey, T. S. Wallis, G. J. Clarke, K. J. Worton, D. C. Candy, and J. Stephen.** 1988. An electron microscopic investigation of time-related changes in the intestine of neonatal mice infected with murine rotavirus. J. Pediatr. Gastroenterol. Nutr. **7:**236–248.
35. **Pearce-Pratt, R., D. Malamud, and D. M. Phillips.** 1994. Role of the cytoskeleton in cell-to-cell transmission of human immunodeficiency virus. J. Virol. **68:**2898–2905.
36. **Petrie, B. L., H. B. Greenberg, D. Y. Graham, and M. K. Estes.** 1984. Ultrastructural localization of rotavirus antigens using colloidal gold. Virus Res. **1:**133–152.
37. **Ploubidou, A., and M. Way.** 2001. Viral transport and the cytoskeleton. Curr. Opin. Cell Biol. **13:**97–105.
38. **Poruchynsky, M. S., and P. H. Atkinson.** 1991. Rotavirus protein rearrangements in purified membrane-enveloped intermediate particles. J. Virol. **65:** 4720–4727.
39. **Prasad, B. V., J. W. Burns, E. Marietta, M. K. Estes, and W. Chiu.** 1990. Localization of VP4 neutralization sites in rotavirus by three-dimensional cryo-electron microscopy. Nature **343:**476–479.
40. **Prasad, B. V., G. J. Wang, J. P. Clerx, and W. Chiu.** 1988. Three-dimensional structure of rotavirus. J. Mol. Biol. **199:**269–275.
41. **Putnam, A. J., J. J. Cunningham, B. B. Pillemer, and D. J. Mooney.** 2003. External mechanical strain regulates membrane targeting of Rho GTPases by controlling microtubule assembly. Am. J. Physiol. Cell Physiol. **284:**C627–C639.
42. **Revenu, C., R. Athman, S. Robine, and D. Louvard.** 2004. The co-workers of actin filaments: from cell structures to signals. Nat. Rev. Mol. Cell Biol. **5:**635–646.
43. **Roncarati, R., and D. Knebel-Morsdorf.** 1997. Identification of the early actin-rearrangement-inducing factor gene, arif-1, from *Autographa californica* multicapsid nuclear polyhedrosis virus. J. Virol. **71:**7933–7941.
44. **Rosso, S., F. Bollati, M. Bisbal, D. Peretti, T. Sumi, T. Nakamura, S. Quiroga, A. Ferreira, and A. Caceres.** 2004. LIMK1 regulates Golgi dynamics, traffic of Golgi-derived vesicles, and process extension in primary cultured neurons. Mol. Biol. Cell **15:**3433–3449.
45. **Salim, A. F., A. D. Phillips, J. A. Walker-Smith, and M. J. Farthing.** 1995. Sequential changes in small intestinal structure and function during rotavirus infection in neonatal rats. Gut **36:**231–238.
46. **Sapin, C., O. Colard, O. Delmas, C. Tessier, M. Breton, V. Enouf, S. Chwetzoff, J. Ouanich, J. Cohen, C. Wolf, and G. Trugnan.** 2002. Rafts promote assembly and atypical targeting of a nonenveloped virus, rotavirus, in Caco-2 cells. J. Virol. **76:**4591–4602.
47. **Sawtell, N. M., A. L. Hartman, and J. L. Lessard.** 1988. Unique isoactins in the brush border of rat intestinal epithelial cells. Cell Motil. Cytoskeleton **11:**318–325.
48. **Scheel, J., R. Matteoni, T. Ludwig, B. Hoflack, and T. E. Kreis.** 1990. Microtubule depolymerization inhibits transport of cathepsin D from the Golgi apparatus to lysosomes. J. Cell Sci. **96:**711–720.
49. **Schevzov, G., C. Lloyd, and P. Gunning.** 1992. High level expression of transfected beta- and gamma-actin genes differentially impacts on myoblast cytoarchitecture. J. Cell Biol. **117:**775–785.
50. **Simon, K. O., P. A. Whitaker-Dowling, J. S. Youngner, and C. C. Widnell.** 1990. Sequential disassembly of the cytoskeleton in BHK21 cells infected with vesicular stomatitis virus. Virology **177:**289–297.
51. **Tihova, M., K. A. Dryden, A. R. Bellamy, H. B. Greenberg, and M. Yeager.** 2001. Localization of membrane permeabilization and receptor binding sites on the VP4 hemagglutinin of rotavirus: implications for cell entry. J. Mol. Biol. **314:**985–992.
52. **Tyska, M. J., and M. S. Mooseker.** 2002. MYO1A (brush border myosin I) dynamics in the brush border of LLC-PK1-CL4 cells. Biophys. J. **82:**1869–1883.
53. **Tyska, M. J., and M. S. Mooseker.** 2004. A role for myosin-1A in the localization of a brush border disaccharidase. J. Cell Biol. **165:**395–405.
54. **van Wijk, E., E. Krieger, M. H. Kemperman, E. M. De Leenheer, P. L. Huygen, C. W. Cremers, F. P. Cremers, and H. Kremer.** 2003. A mutation in the gamma actin 1 (ACTG1) gene causes autosomal dominant hearing loss (DFNA20/26). J. Med. Genet. **40:**879–884.
55. **Vellenga, L., H. J. Egberts, T. Wensing, J. E. van Dijk, J. M. Mouwen, and H. J. Breukink.** 1992. Intestinal permeability in pigs during rotavirus infection. Am. J. Vet. Res. **53:**1180–1183.
56. **von Schwedler, U. K., M. Stuchell, B. Muller, D. M. Ward, H. Y. Chung, E. Morita, H. E. Wang, T. Davis, G. P. He, D. M. Cimbora, A. Scott, H. G. Krausslich, J. Kaplan, S. G. Morham, and W. I. Sundquist.** 2003. The protein network of HIV budding. Cell **114:**701–713.
57. **Watts, B. A., III, T. George, and D. W. Good.** 2005. The basolateral NHE1 Na+/H+ exchanger regulates transepithelial HCO3-absorption through actin cytoskeleton remodeling in renal thick ascending limb. J. Biol. Chem. **280:**11439–11447.
58. **Winder, S. J., and K. R. Ayscough.** 2005. Actin-binding proteins. J. Cell Sci. **118:**651–654.
59. **Yonemura, S., and S. Tsukita.** 1999. Direct involvement of ezrin/radixin/moesin (ERM)-binding membrane proteins in the organization of microvilli in collaboration with activated ERM proteins. J. Cell Biol. **145:**1497–1509.
60. **Zicha, D., I. M. Dobbie, M. R. Holt, J. Monypenny, D. Y. Soong, C. Gray, and G. A. Dunn.** 2003. Rapid actin transport during cell protrusion. Science **300:**142–145.